Front. Optoelectron. 2017, 10(4): 388–394
https://doi.org/10.1007/s12200-017-0747-z

RESEARCH ARTICLE

Waveform LiDAR signal denoising based on connected domains

Liyu SUN, Zhiwei DONG, Ruihuan ZHANG, Rongwei FAN, Deying CHEN (✉)

National Key Laboratory of Science and Technology on Tunable Laser, Harbin Institute of Technology, Harbin 150001, China

Abstract The streak tube imaging light detection and ranging (LiDAR) is a new type of waveform sampling laser imaging radar whose echo signals are stripe images with a high frame rate. In this study, the morphological and statistical characteristics of stripe signals are analyzed in detail. Based on the concept of mathematical morphology denoising, connected domains are constructed in a noise-containing stripe image, and the noise is removed using the difference in connected domains area between signals and noises. It is shown that, for stripe signals, the proposed denoising method is significantly more efficient than Wiener filtering.

Keywords stripe signal, connected domain, denoising

1 Introduction

Light detection and ranging (LiDAR) is widely applied in mapping fields due to its high precision and excellent distance gating capability. However, the working mechanism of most LiDAR systems is based on a single point, i.e., the system detects only one echo signal per working period, which limits the efficiency of the whole system [1, 2]. The streak tube imaging LiDAR (STIL) is a type of full-waveform sampling LiDAR system whose echo signal contains full waveform information of the target, and it can gather hundreds of waveform echo signals in one working period [3–5]. It has been demonstrated that STIL is a satisfactory solution for achieving a highly efficient terrain detection, and it is also promising for underwater target detection [6–9]. However, the processing of mass waveform signals collected by an STIL system is a challenge that has to be addressed.

In recent years, the research on STIL systems is focused on the detection ability and performance index [10–14]. Processing methods for mass data collected by STIL are still lacking, which is a key bottleneck for the development of full-waveform sampling LiDAR. In this study, a denoising method for stripe waveform signals gathered by STIL is proposed. Compared with the traditional Wiener filtering, the proposed connected domain denoising method is more efficient and provides a satisfactory denoising effect.

Received August 4, 2017; accepted October 12, 2017

E-mail: dychen@hit.edu.cn

2 Experiments and principles

Figure 1 shows the diagram of a typical streak tube. When the echo laser pulse exposes the slit of the photocathode, the target echo signal is converted into electrons. This electron beam is then accelerated to the phosphor anode by the applied voltage between the cathode and anode. During the accelerated motion, the electrons are deflected under different angles using a pair of sweep plates (which produce a linear ramp voltage), and form luminous points on a phosphor screen, which provides time information. Then, the phosphor screen image is recorded by a charge coupled device (CCD) with high temporal and spatial resolution.

The typical STIL echo signals are stripe images containing temporal and spatial information, as shown in Fig. 2. Each row vector of the image represents a time-resolved channel, which reveals the time (distance) information, while each column reveals the azimuth (spatial) information of the laser [15,16]. Using such images, we can obtain the target location information, as the stripe signal represents the echo of the target.

Wiener filtering is one of the universal denoising methods for LiDAR echo signals [17]. The mathematical model of the Wiener filtering is described as follows [18]:

$$g(x,y) = \mu + \frac{\sigma^2 - v^2}{\sigma^2}[f(x,y) - \mu], \tag{1}$$

where μ and σ^2 represent the local mean and variance

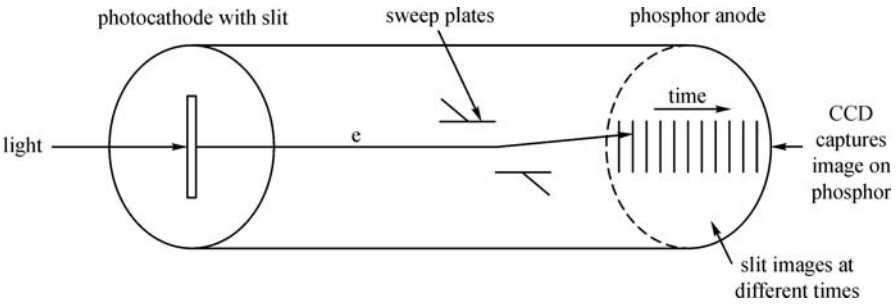

Fig. 1 Diagram of typical streak tube

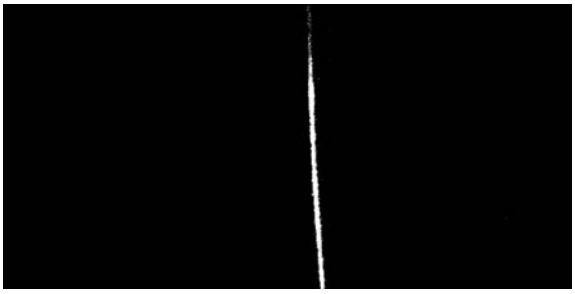

Fig. 2 Original stripe image

(around each pixel), respectively, while v^2 is the variance of the noise.

This method is efficient when applied to conventional LiDAR echo signals. However, the above method is not efficient when applied to the waveform sampling signal due to the relatively complex computational procedures. In this paper, we propose a new morphology denoising method based on connected domains, and it is shown that this method is suitable for waveform sampling stripe signal denoising.

Connectivity means that for any two points in a collection, there is a connection path between them that belongs entirely to the collection. For data images, connectivity is divided into four adjacencies and eight adjacencies. Four adjacencies are the four directions: up, down, left, and right; when moving from a pixel along these directions any other pixel location is reached. Eight adjacencies are the eight directions: up, down, left, right, upper left, upper right, bottom left, and bottom right; when moving from a pixel along these directions any other pixel location is reached [19]. In this study, the eight adjacencies method was applied.

The labeling of connected domains, i.e., assigning a unique number to each connected domain, is the key of this method. In this study, we adopt the method of pixel scanning in order to label the connected domains. The principle of labeling connected domains can be described as follows [20]:

$$\mathrm{merge}(x,y)=\begin{cases}\mathrm{merge}(x-1,y), & \text{if } f(x,y)=f(x-1,y) \text{ and } f(x,y)\neq f(x,y-1),\\ \mathrm{merge}(x,y-1), & \text{if } f(x,y)\neq f(x-1,y) \text{ and } f(x,y)=f(x,y-1),\\ \mathrm{merge}(x,y-1), & \text{if } f(x,y)=f(x-1,y) \text{ and } f(x,y)=f(x,y-1),\\ \text{newlabel}, & \text{if } f(x,y)\neq f(x-1,y) \text{ and } f(x,y)\neq f(x,y-1),\end{cases} \tag{2}$$

where $f(x,y)$ is the gray value of the input image, while $\mathrm{merge}(x,y)$ is the connected domain tag of $f(x,y)$.

The flow diagram of the connected domain method is shown in Fig. 3.

First, we constructed connected domains in the original input stripe image using eight adjacencies, then labeled the connected domains as: 1, 2, 3,…,n, and calculated the area of each connected domain. Taking into account that the area of the signal is significantly larger than that of the noise, it is not difficult to distinguish the signals from the noise, by defining an appropriate threshold area. Therefore, a connected domain whose area is below the threshold area is considered as a noise. The pixel coordinates of the noise can be simultaneously obtained; similarly, the coordinates of the signals can be obtained.

Then, we introduced a matrix $\boldsymbol{A}$, which has the same size as that of the original stripe image. According to the coordinates of the signals and noise in the stripe image, we set the corresponding values of the signals to one, while the values of the noise to zero. When $\boldsymbol{A}$ is multiplied with the corresponding matrix of the original stripe image, a denoised matrix is obtained, and the noise in the stripe image can be removed.

The denoising effect can be evaluated using the signal-to-noise ratio (SNR), the correlation coefficient (r), and the measure of dispersion (i.e., std), defined as follows:

$$\mathrm{SNR}=10\lg\left(\frac{S}{N}\right), \tag{3}$$

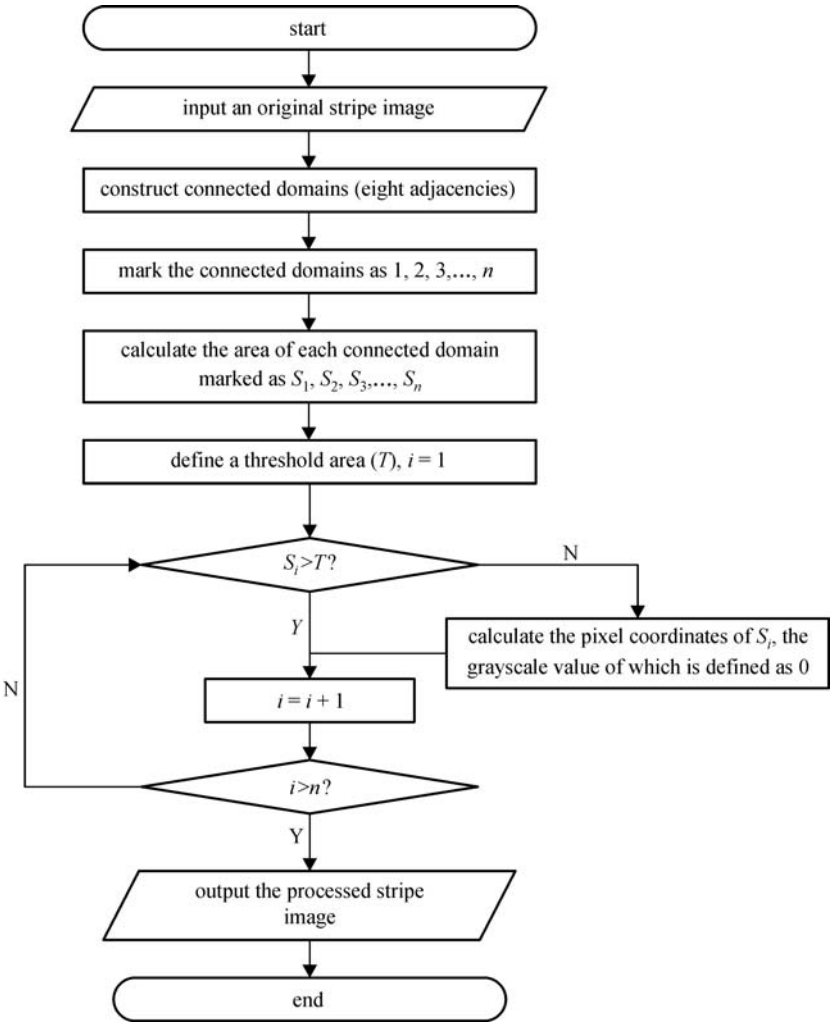

Fig. 3 Flow diagram of connected domain method

$$r = \frac{\Sigma_m \Sigma_n \left(I^A_{mn} - \overline{I^A}\right)\left(I^B_{mn} - \overline{I^B}\right)}{\sqrt{\left[\Sigma_m \Sigma_n \left(I^A_{mn} - \overline{I^A}\right)^2\right]\left[\Sigma_m \Sigma_n \left(I^B_{mn} - \overline{I^B}\right)^2\right]}}, \quad (4)$$

$$\text{std} = \sqrt{\frac{1}{N}\Sigma_{i=1}^{N}\left(h_i - \overline{h}\right)^2}. \quad (5)$$

In Eq. (3), S is the intensity of the signal, while N represents the intensity of the noise. In Eq. (4), I^A is the intensity of the original image, while I^B represents the intensity of the denoised image. In Eq. (5), N is the number of points, while h represents the height of each point in the point cloud.

The SNR characterizes the denoising effect, while the correlation coefficient shows the degree of correlation of signals before and after denoising, which is very important for a detailed retention of the LiDAR targets. The dispersion can also characterize the denoising effect, as it is sensitive to the rudimental noise in the stripe image.

3 Results and discussion

3.1 Selection of threshold area

Choosing an appropriate threshold area is of significant importance for the connected domain method. According to the connected domain area graph of a typical stripe image (Fig. 4), the area of the signal is $\sim$ 1400, while for most of the noise it is below 200; the difference is significant.

In order to obtain the mean of SNR and r, and find the appropriate threshold area, we consider threshold area values of 20, 50, 100, 200, 300, and 500, and study a set of 1000 stripe images. As shown in Fig. 5, the SNR increases rapidly when the threshold area is less than 200, and gradually increases when the threshold area is more than 200; the correlation coefficient decreases monotonously when the threshold area increases. In order to obtain a high value of SNR, and a correlation coefficient larger than 0.990, we selected 200 as the threshold area.

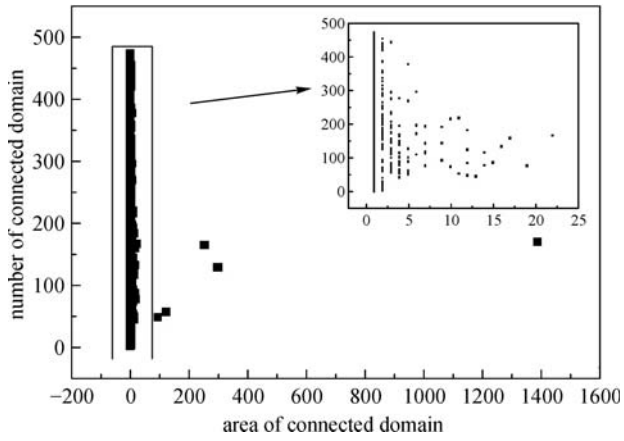

Fig. 4 Connected domain area graph

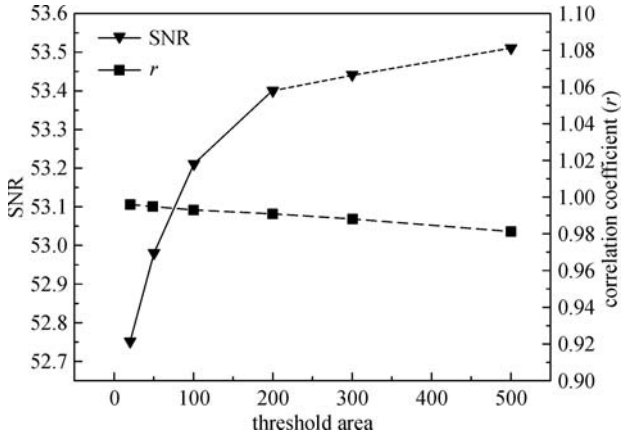

Fig. 5 Denoised results for different threshold area

3.2 Comparison of denoised results

The denoised results obtained by Wiener filtering and connected domain method are shown in Figs. 6(a) and 6 (b), respectively. In Fig. 6(a), the background noise is almost removed; however some details of the signal are lost. For example, the top part (present in the original echo image shown in Fig. 2) of the stripe is eliminated. Moreover, the denoised signal is smoother and the edges become blurry. In contrast, as shown in Fig. 6(b), when the denoising is performed using the connected domain method, the random shot noise in the background disappears, and the shape of the stripe signal remains unaffected, which is important for the processing of LiDAR signals.

These two denoising methods are quantitatively compared in Table 1. The time required to process 1000 stripe images by Wiener filtering is 35 s. When the connected domain method is used the processing time is only 16 s, hence the efficiency (for denoising of stripe signals) of the connected domain method is almost twice that of Wiener filtering. This is very important for the processing of waveform sampling echo signals. The mean SNR values of the signals denoised by Wiener filtering and connected domain method were 43 and 53, respectively, which suggests that the denoising effect is better when the connected domain method is used. In addition, the connected domain method has a better correlation coefficient compared to that of the Wiener filtering, as shown in Fig. 6. This implies that the target details are better preserved when the connected domain method is used.

3.3 Comparison of point clouds

The conventional LiDAR output is a point cloud data and its elevation map. Figure 7 shows the elevation maps of typical building targets before denoising as well as after denoising by Wiener filtering and by the connected domain method. There are massive noise points around the buildings in Fig. 7(a), while they are almost vanished in Figs. 7(b) and 7(c).

In order to investigate the specific effects of these two denoising methods using elevation maps, we chose the flat ground between the upper two big buildings (shown in Fig. 7). The results for the flat ground are shown in Fig. 8. It can be seen that there are massive noise points around the flat ground in Fig. 8(a), while they are almost vanished in Figs.

Fig. 6 Denoised results of waveform sampling stripe signals. (a) Denoised result of Wiener filtering; (b) denoised result of connected domain method

Table 1 Comparison of different denoising methods

	denoising time/s	mean of r	mean of SNR
connected domain method	16	0.99	53
Wiener filtering	35	0.96	43

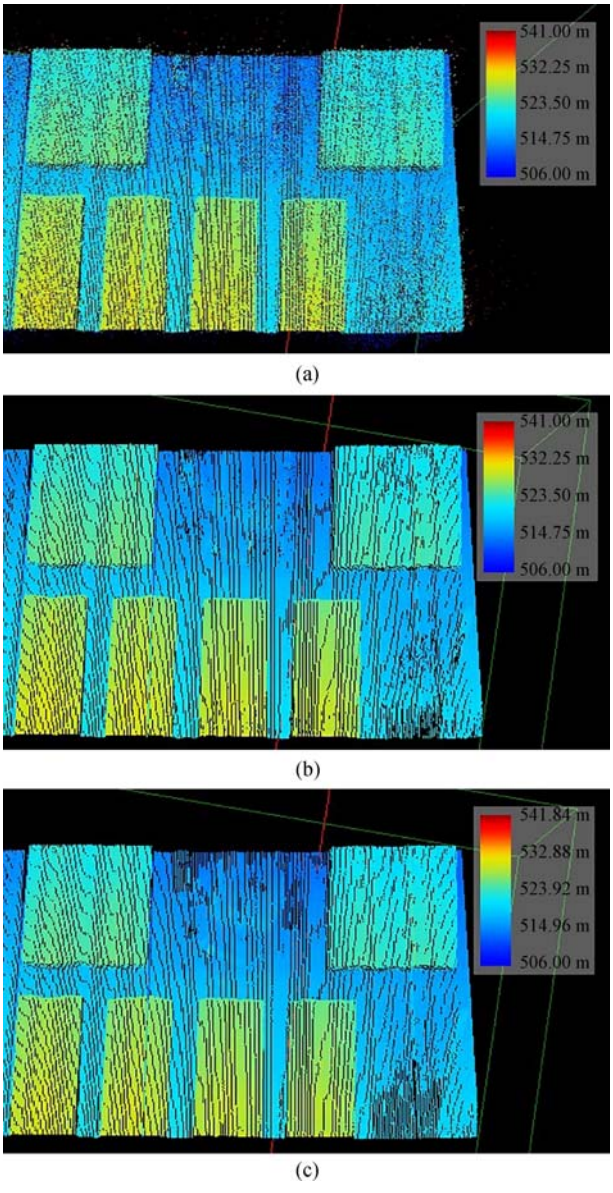

Fig. 7 Elevation maps of buildings. (a) Original points cloud before denoising; (b) denoised by Wiener filtering; (c) denoised by connected domain method

8(b) and 8(c). It can be noticed that some of the discrete points are present in Fig. 8(b), while most of them do not appear in Fig. 8(c).

The quantitative results of the elevation maps are shown in Table 2. The dispersions of the point clouds in Fig. 8(a)–8(c) are 10.02, 2.54, and 2.39, respectively. It is obvious that the dispersion for Fig. 8(c) is the smallest which indicates that the connected domain method provides better denoising compared to that of the Wiener filtering. The efficiency of the denoising algorithm can be also evaluated by the point density. As shown in Table 2, the point densities of Figs. 8(a)–8(c) are 4.57, 3.59, and 2.99, respectively. The point densities of Figs. 8(b) and 8(c) are smaller than that of Fig. 8(a), which indicates that both

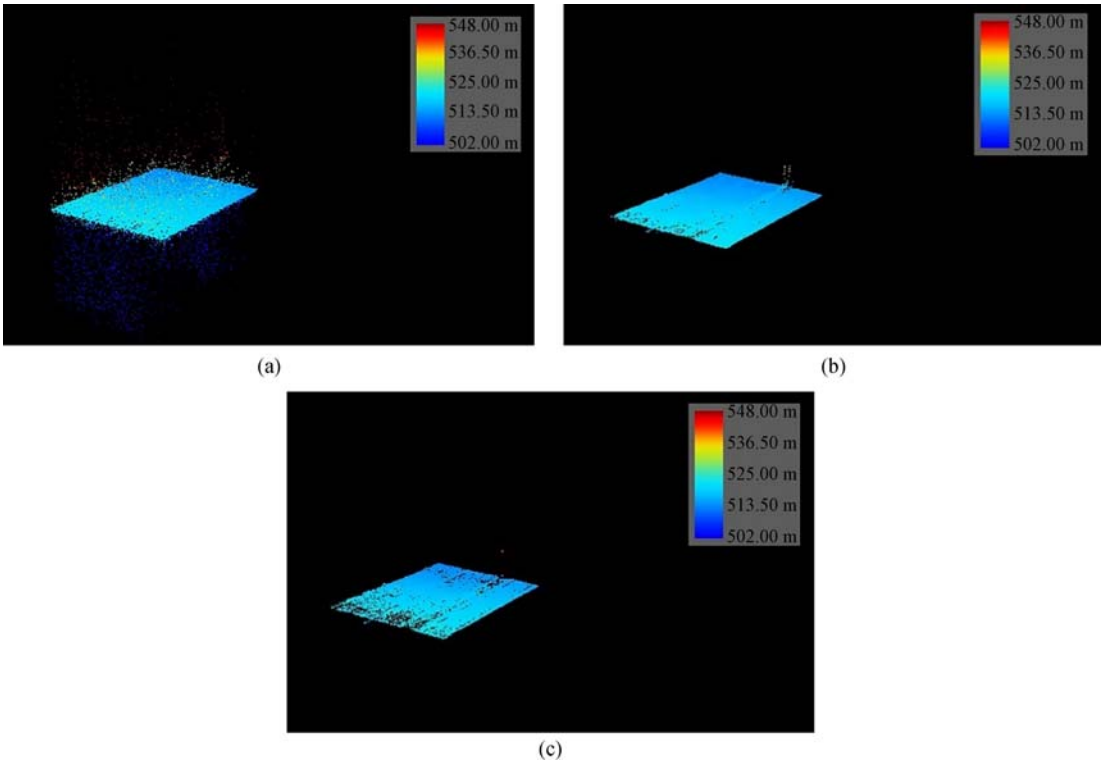

Fig. 8 Elevation maps of flat ground. (a) Original points cloud before denoising; (b) denoised by Wiener filtering; (c) denoised by connected domain method

Table 2 Dispersion and point density of flat ground in points cloud

	not denoised	Wiener filtering	connected domain method
dispersion	10.02	2.54	2.39
point density/m^2	4.57	3.59	2.99

Wiener filtering and connected domain method achieve a significant denoising. Furthermore, the point density of Fig. 8(c) is the smallest, hence the connected domain method provides better results.

4 Conclusions

In this study, a novel denoising algorithm based on connected domains was applied in order to process waveform sampling LiDAR echo signals. Compared with the conventional Wiener filtering, the proposed method has a higher efficiency and provides a satisfactory denoising of stripe signals. Our results confirm that the connected domain method is promising for applications in denoising of STIL echo signals.

Acknowledgements The authors gratefully acknowledge the financial support from the National Natural Science Foundation of China (Grant No. 11004042), National Key Scientific Instrument and Equipment Development Projects (No. 2012YQ040164), National Key Laboratory of Science and Technology on Tunable laser, Space Science and Technology Fund and Science Funds of Heilongjiang Province (No. F2016015).

References

1. Li Q, Wang Y, Wang Q, Li Z. Noise suppression algorithm of coherent ladar range image. Acta Optica Sinica, 2005, 25(05): 581–584
2. Li Q, Wang Q, Li Z, Li L, Jiang L. Image processing on laser imaging radar. Chinese Journal of Lasers, 2002, A29(09): 826–828
3. Gleckler A D, Gelbart A, Bowden J M. Multispectral and hyperspectral 3D imaging Lidar based upon the multipleslit streak tube imaging lidar. Proceedings of the Society for Photo-Instrumentation Engineers, 2001, 4377: 328–335
4. Gleckler A D, Gelbart A. Three-dimensional imaging polarimetry. Proceedings of the Society for Photo-Instrumentation Engineers, 2001, 4377: 175–185
5. Nevis A J. Automated processing for streak tube imaging lidar data. Proceedings of the Society for Photo-Instrumentation Engineers, 2003, 5089: 119–129
6. Gelbart A, Redman B C, Light R S, Schwartzlow C A, Griffis A J.

Flash lidar based on multiple-slit streak tube imaging lidar. Proceedings of the Society for Photo-Instrumentation Engineers, 2002, 4723: 9–18
7. Sun J F, Liu D, Ge M D, Wang Q. Image pre-processing algorithm of underwater target for streak tube imaging lidar. Chinese Journal of Lasers, 2013, 40(07): 211–214
8. Sheng Y P, Sun J F, Xu D W. Application analysis of short-range ocean surface monitoring for streak tube imaging lidar. Electro-Optic Technology Application, 2012, (1): 34–36,70
9. Sun J F, Gao J, Wei J S, Wang Q. Research development of underwater detection imaging based on streak tube imaging lidar. Infrared and Laser Engineering, 2010, 39(05): 811–814
10. Li S N, Liu J B, Guang Y H, Zang J H, Wang Q. Maximum acquisition range calculation for multi-wavelength streak tube image lidar. Acta Photonica Sinica, 2007, 36(S1): 106–109
11. Wei J S, Wang Q, Sun J F, Gao J. Experiment of four-dimensional imaging with single-slit streak tube lidar. Chinese Journal of Lasers, 2010, 37(5): 1231–1235
12. Zhang J H, Li S N, Wang Q, Liu J B. Noise analyzing and processing of streak image for streak tube imaging lidar. Acta Photonica Sinica, 2008, 37(8): 1533–1538
13. Dong Z W, Zhang R H, Zhang W B. Noise features in streak tube lidar echo signal. Acta Optica Sinica, 2016, 36(09): 296–300
14. Dong Z W, Zhang W B, Fan R W. Streak tube principle lidar imaging simulation and experiment Infrared and Laser Engineering. Infrared and Laser Engineering, 2016, 45(07): 100–104
15. Gleckler A. Streak tube imaging lidar for electro-optic identification. In: Proceedings of 4th International Symposium on Technology and the Mine Problem, 2001
16. Redman B C, Griffis A J, Schibley E B. Streak tube imaging lidar (STIL) for 3-D imaging of terrestrial targets. In: Proceedings of the MSS Specialty Group on Active E-O Systems, 2000
17. Bian X D. Research on stripe image processing for three-dimensional laser mapping. Dissertation for the Master Degree. Harbin: Harbin Institute of Technology, 2015, 20–21
18. Lim J S. Two-Dimensional Signal and Image Processing. Englewood Cliffs, NJ: Prentice Hall, 1990
19. Fan J M. Design and application of the labeling algorithm of 8-adjacent connecting area for massive gray scale images. Dissertation for the Master Degree. Kaifeng: Henan University, 2015
20. Suzuki K, Horiba I, Sugie N. Linear-time connected-component labeling based on sequential local operations. Computer Vision and Image Understanding, 2003, 89(1): 1–23

Liyu Sun, master in Harbin Institute of Technology. His current research is laser remote sensing and image information processing.

Zhiwei Dong, professor in Harbin Institute of Technology. His research interests focus on LiDAR and laser spectra.

Ruihuan Zhang, Doctor in Shanghai Jiao Tong University. She got her master degree at Harbin Institute of Technology in 2016. Her current research is optical fiber communication and silicon-based optical passive devices.

Rongwei Fan, professor in Harbin Institute of Technology. His research interests focus on LiDAR and laser technology.

Deying Chen, professor in Harbin Institute of Technology. His research interests focus on LiDAR and laser technology.